



PREPARATION AND INVESTIGATION OF THE MECHANICAL BEHAVIOR OF TEMPORARY ZINC ALLOYS AS BIODEGRADABLE IMPLANTS

Ban A. Okab¹, Jassim M. Salman², and Nabaa Sattar Radhi³

¹ College of Engineering Materials, University of Babylon, Babylon 51013, Iraq,
Email:mat599.ban.abad@student.uobabylon.edu.iq

² College of Engineering Materials, University of Babylon, Babylon 51013, Iraq,
Email:mat.jassim.mohammed@uobabylon.edu.iq.

³ College of Engineering Materials, University of Babylon, Babylon 51013, Iraq,
Email:mat.nabaa.sattar@uobabylon.edu.iq.

<https://doi.org/10.30572/2018/KJE/170136>

ABSTRACT

The development of Mg and Fe based biomaterials in the past decade has been extensively studied as biodegradable material for medical applications. The development of this material is limited in terms of its suitability for clinical applications. Zn-based alloys began to be an alternative to be studied as a substitute for Mg and Fe based biomaterials. Zn-based alloys have a moderate degradation rate but have low mechanical properties, so other elements need to be added to improve their mechanical properties. In this study, the added elements are silver and Zirconium. Compared to pure Zinc the mechanical strength was enhanced significantly for all tested Zinc alloys. Accordingly, we design four alloys (pure Zinc, Zinc+0.4 Silver, Zinc +0.4 Zirconium and Zinc + 0.4 Silver+ 0.4 Zirconium) wt.%. The alloys are developed by stir casting process and homogenized at 280 C° for 1 hour. The Vickers hardness and compression tests of alloys were investigated. The hardness value of zinc based alloy is (64.28 kg/mm²) increased to (100.53kg/mm²) for (Zn-Ag-Zr) alloy, and the improvement percentage of hardness to (Zn-Ag-Zr) alloy arrived to maximum (56.3%). In addition, the compression value of zinc based alloy is (165.95 MPa) increased to (307.76 MPa) for (Zn-Ag-Zr) alloy, and the improvement percentage of compression test to (Zn-Ag-Zr) alloy is (85.45%). So (Zn-Ag-Zr) alloy is considered the best alloy to enhance compressive strength where achieve higher improvement percentage.



KEYWORDS

Bioresorbable metals, Mechanical properties, Biodegradable metals, Zn-based alloy, Orthopedic implants, Microstructure.

1. INTRODUCTION

With the development of bioresorbable or biodegradable metallic materials, permanent orthopedic implants, cardiovascular devices, and scaffolds for tissue engineering now have a viable substitute (Sabir et al., 2009; Yin et al., 2019; Jasim & Radhi, 2024). Before slowly disintegrating in the body and generating innocuous corrosion products, biodegradable materials can retain the anticipated mechanical integrity during the healing process. Thus, biodegradable materials reduce the necessity for a second operation to remove the device and the problems brought on by the immune response to the implant and prolonged exposure (Hermawan, 2018; Radhi et al., 2022). This idea has led to a lot of studies on alloys made of magnesium, iron, and, more recently, Zinc. Several factors have prevented the widespread use of metallic materials in bioresorbable implants: Magnesium alloys were previously demonstrated to be non-toxic for human body and suitable as biodegradable material, but have a tendency to excessively deteriorate rapidly, and hydrogen evolution occurs along with the high rate of corrosion (Gu et al., 2009; Zheng et al., 2014). However, iron alloys tend to deteriorate too slowly and have lower biocompatibility (Pierson et al., 2012). The creation of biomaterials based on magnesium and iron during the last 10 years has been thoroughly investigated as a biodegradable substance for use in medicine. Nevertheless, despite this material system's substantial growth, its usefulness for clinical applications is limited or stagnates (Ma et al., 2015; Haleem et al., 2024). Zinc is a novel kind of biodegradable metal, after magnesium and iron, due to its high decomposition rate and biocompatibility. And because of the standard corrosion potential of Zinc is (-0.762 VSCE), Zinc exhibits a lower corrosion rate than the Mg (-2.372 VSCE) and Fe (-0.440 VSCE) (Okab et al., n.d.). Hence, Zn, its alloys and composites are emerging as a new class of BMs and are considered promising alternatives to Mg-based and Fe-based BMs for biomedical applications, particularly orthopedic regeneration, and cardiovascular therapy (Kabir et al., 2021). Zinc is one of the most important elements in the human body, which contains over 300 proteins and enzymes. Zinc ions can still be incorporated into the body's metabolic processes after being broken down from the implant without having any harmful side effects (Liu et al., 2016). Other biomaterials made of zinc-based alloys have the benefit of a moderate rate of deterioration due to their passive layer's moderate durability, and casting zinc-based alloys is made easier by their low melting point and low chemical reactivity (Dargusch, 2019). Biodegradable Zn metal possesses extremely good biocompatibility and biodegradability, but low mechanical specifications limited its applications in biomedical (Kong et al., 2023), insufficient for most medical applications due to low strength (UTS ~ 30 MPa) and plasticity ($< 0.25\%$) characteristics (Levy et al., 2017), as

well as lower values for tolerance of organisms to Zn led to excessive release of (Zn^{2+}) in implants materials during the degradation and caused severe cytotoxicity in the vitro and delayed of bone osseointegration in the vivo (Zhang et al., 2023). Therefore, developing zinc with sufficient hardness and high strength is one of main goals of the metallurgical engineering, one of most powerful approach to improve mechanical performance of the metal is the addition of alloying elements (Levy et al., 2017), that could recommended as efficient method for enhancing mechanical features. Alloying elements are utilized as good tool to significantly enhancement the performance of Zinc (Kong et al., 2023). Many studies found that the alloying elements formed the intermetallic compounds, not only affect the plastic deformation ability and strength of the Zn alloys but also influence on their property of degradation and cytotoxicity (Zhang et al., 2023). Alloying elements, such as Ag and Zr, can be added to Zn-based materials to improve their mechanical properties. Zirconium (Zr), an element with potential biocompatibility and bioneutrality, is also one of the elements with low systemic toxicity. However, its use as an alloying element for Zn-based materials has not received much attention (Ghani Fahmi et al., 2020). Zr is not dissolved in Zn matrix and precipitates formed are identified as $Zn_{22}Zr$. Insoluble Zr inhibits the growth of grain size and result in finer grain and smaller sizes, this in turn increases the hardness (Okamoto, 2007). Ag is also suggested as an alloying element since it maintains biocompatibility while enhancing mechanical qualities (Mostaed et al., 2017). Potential cardiovascular implants would be very interested in Ag being added as the alloying element to Zinc or Zinc alloy systems (Mostaed et al., 2018), and studies have been reported in Zn alloys and reached that the improved ductility, strength, and microstructure for the applications of medical implants (Guillory et al., 2022), also confirmed to possess super plasticity as well as high mechanical strength, and suggests promising new class of biodegradable metals (Xiao et al., 2021). The essential objective of the current work is the fabrication of a ternary Zn alloy by introducing silver and zirconium alloying elements by stir casting method to address the drawbacks of the pure Zinc alloy.

2. EXPERIMENTAL PART

2.1. Preparation of Specimens

To prepare, the alloys (pure Zinc, Zinc 0.4 wt.% Silver, Zinc 0.4 wt.% Zirconium and Zinc 0.4 wt.% Silver 0.4 wt.% Zirconium) by stir casting method, the following steps are typically involved: The materials used in the research are pure Zinc of purity (99.99%) were obtained from mineral madencilik/turkey, pure Zr of purity (99.5%) were obtained from murat geri Dönüşüml turkey and pure Ag of purity (99.0%) were obtained from china. First, the

approximate weight of the casting is determined by the approximate density of the casting 7.5g/cm³ close to the density of Zinc. The weight of all zirconium and silver is extracted according to the added ratios, taking into account the combustion of Zirconium. The zinc is a form of the bulk and is placed in the melting point, heated until it melts (approximately 500C°) and then poured in the mold, let it cool and then extract the pure zinc. zirconium is wrapped in powder form with Zinc foil to reduce its combustion process, as it is very sensitive to combustion.

Second, the silver is in the form of bulk, melted Zinc and added Silver partially with mixing to ensure their homogeneity in the melt after turning off the oven to avoid burning the Zinc. After that all the Zinc is melted, the slag is removed and the molten is poured into a cast iron mold heated for heat 300 C°. The diameter of the mold is 12 mm and the length is 220 mm, let it cool and then extract the alloy.

As for the Zinc-Zirconium alloy, the Zinc is melted first and then the Zirconium is added to the molten after heating the Zirconium to get rid of the possible moisture where the heating is about 200 C°. After adding Zirconium, the molten is mixed well and then poured into the mold after removing the slag and letting it cool to produce the alloy.

Finally, the ternary Zinc-Silver-Zirconium alloy was fabricated by melting Zinc in a small amount then added Silver and mixing, then all the Zinc was introduced, and after that, the Zirconium was added. To avoid thermal shock, the mold should be preheated, then the molten metal was poured into a mold and allowed to solidify. The alloys are allowed to cool naturally to room temperature. after that, thermal homogenization process at a temperature (of 280) °C for (1) hour and slow cooling in the furnace. Then, alloys are machined with a lathe machine to produce a disc sample with dimensions of (13 mm) in diameter and (5) mm in thickness, which are used for tests. The casting specimens were ground with SiC paper grits (180, 400, 600, 800, 1000, 1200, 1500 and 2000) and then polished by using a diamond solution (0.5 µm). Then, the samples were washed with distilled water and dried using an electric dryer. The samples were etched at room temperature by (2 g Cr₂O₃, 10 ml distilled water) (Ag- et al., 2015). Chemical analysis was conducted using an X-ray fluorescence (XRF) test at the Ministry of Science and Technology in Baghdad, Iraq. Table 1 shows the chemical analysis of the alloys.

Table 1 Chemical composition of the alloys (wt.%).

Elements (Wt. %)	Zn	Zr	Ag	Cu	Fe	Co
Zn-pure	99.68	-	-	0.0282	0.0214	0.0197
Zn-Zr	99.1	0.35	-	-	0.09	-
Zn-Ag	98.9	-	0.39	0.10	0.12	0.06
Zn-Zr-Ag	98.6	0.35	0.38	0.07	0.2	-

2.2. Tests

Optical microscope model (1280XEQ-MM300TUSB) and Scanning electron microscope (VEGA3SBU) were used to examine the microstructure. X-ray diffraction (XRD) was used for examined the chemical phases analysis of samples. Micro-hardness testing is used to measure the hardness values by Vickers hardness device type (Digital Micro hardness tested HV-1000). The hardness is examined according to (ASTM E384) after 10 seconds of applying a 100 g weight to the test specimen using a square-based diamond indenter. Three readings were reordered for each specimen, and the average value was calculated. The compression test was performed according to ASTM (E9–89a) at room temperature. The specimens' dimensions are (12 mm diameter and 10 mm thickness). They were positioned vertically between the grips to measure compression strength.

3. RESULTS AND DISCUSION

3.1. Microstructure of the alloys

[Fig.1,2](#) indicate the microstructure generated by the material utilized. Because the size and shape of the grains directly affect the material's behavior, metallography can provide a simplified understanding of the connections between the material's microstructure and microscopic characteristics. [Fig.1,2](#) using optical micrographs and SEM images display, at 200x magnification, the microstructure of the etched alloys after the homogenization process evaluating the microstructure of the aforementioned alloys showed the boundaries of the grains and the present phases. Every sample will have a macrostructure, whether amorphous or crystalline. From [Fig.1,2](#) The pure Zn microstructure test findings show that the grain size is quite large, tends to be rough, and consist mainly of one phase the (α - Zn) appear ([Ghani Fahmi et al., 2020](#)). Additionally when adding 0.4 wt.% Ag to Zn, Ag is dissolved in the Zn matrix and because of lower Ag content, no secondary phase appeared ([Wa et al., 2019](#)). After adding 0.4 wt.% Zirconium, two phases, the α Zn phase and the Zn₂₂Zr intermetallic phase, are visible. This is in accordance with the Zn-Zr phase diagram ([Williams et al., 2004](#)), which states that the intermetallic phase Zn₂₂Zr forms around 550°C because zirconium does not dissolve into the Zn matrix at this temperature. These precipitates that do develop are still typically tiny and in smaller quantities. These precipitates are oval or globular in form, and their distribution is uneven; they still only gather in particular parts of the grain boundary ([Ghani Fahmi et al., 2020](#)). As for Zn-0.4 wt.% Zirconium+0.4 wt.% Ag alloy, the microstructure consists of only a single (α - Zn) phase appear ([Wa et al., 2019](#)).

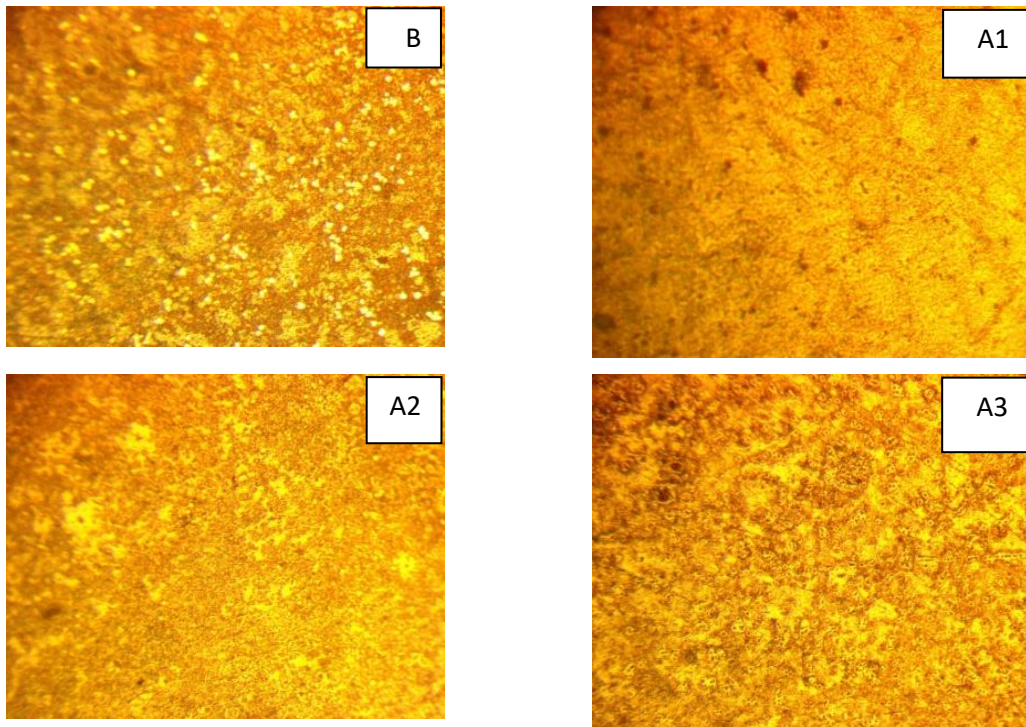


Fig.1. Microstructure of alloys, B :pure Zn alloy , A1: (Zn-0.4 Ag), A2: (Zn-0.4 Zr), A3: (Zn-0.4 Ag-0.4 Zr) wt% with 200x magnification.

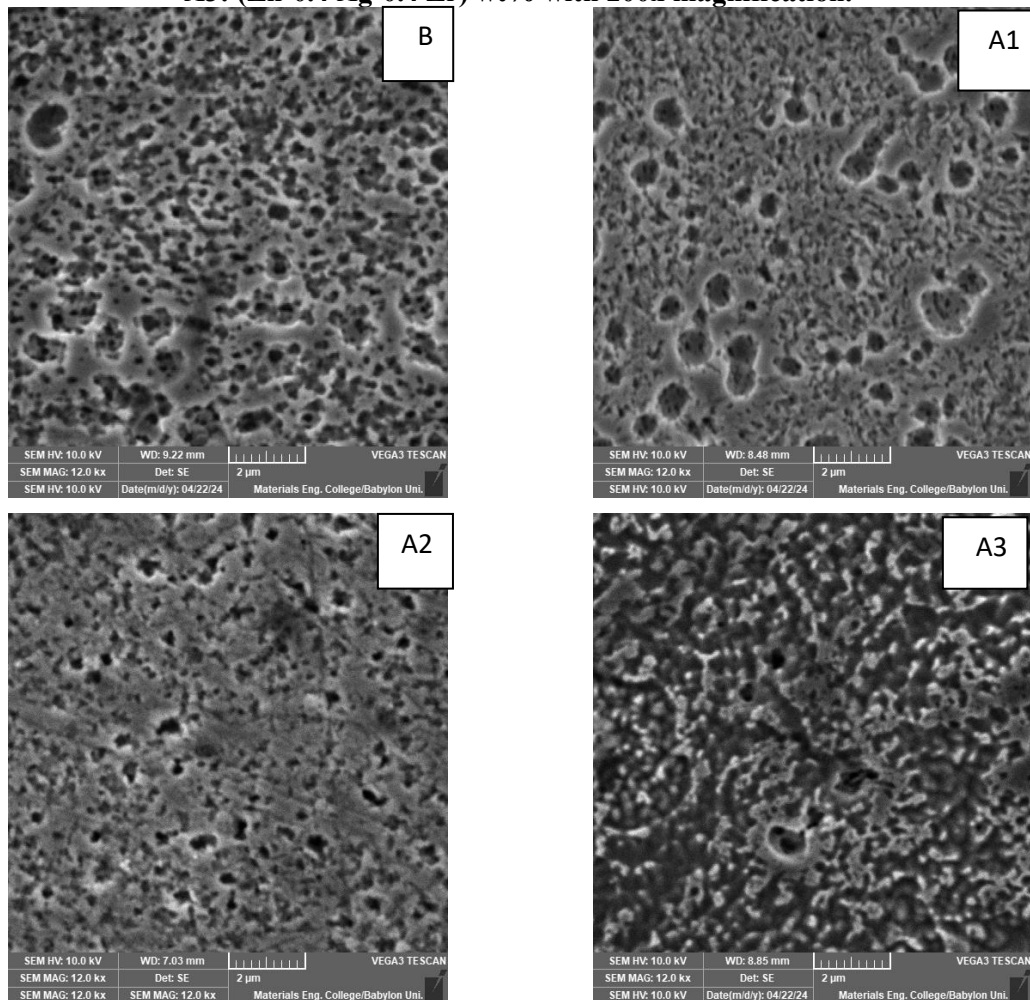
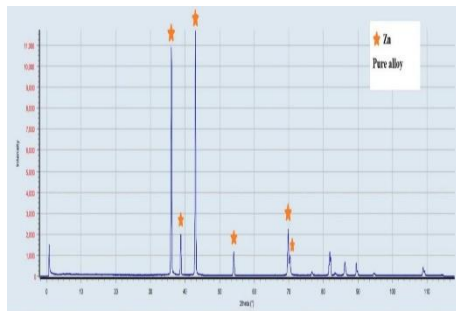


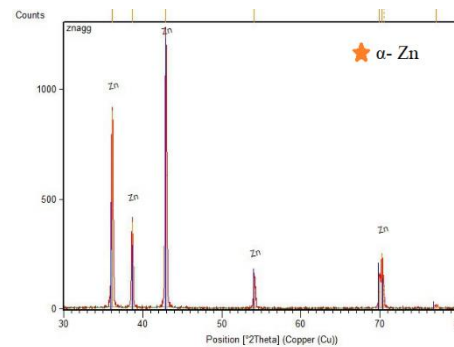
Fig.2. SEM images for alloys, B :pure Zn alloy , A1: (Zn-0.4 Ag), A2: (Zn-0.4 Zr), A3: (Zn-0.4 Ag-0.4 Zr) wt%

3.2. X-ray Diffraction for Alloys

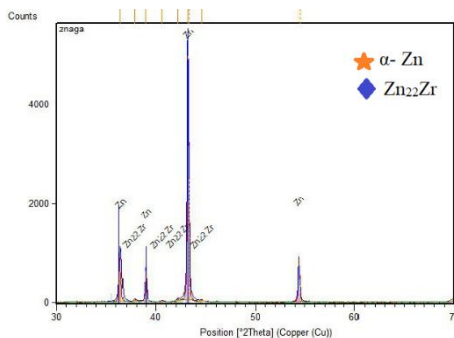
The main objective of X-ray diffraction was to determine the phases present in specimens of the studied Zinc alloy with and without additions because, in general, the mechanical and physical properties of the alloys are affected by phase transition. The pattern of the pure zinc alloy in Fig.3a revealed the alpha phase that matched the card number (010-87-0713). It can be seen that the pure Zinc alloy mainly consists of (α - Zn) which agrees with (Ghani Fahmi et al., 2020). It can be seen that the pure Zinc alloy mainly consists of (α - Zn). In Fig.3b, when 0.4 wt% Ag is added to Zn ,because of lower Ag content and that Ag is dissolved in the Zn matrix the results of XRD analysis similar to pure Zn (α - Zn) (Wa et al., 2019). In Fig.3c, the α -Zn phase and the Zn₂₂Zr intermetallic phase are the two phases that are visible in the Zn-0.4wt% Zr alloy. According to the literature on the Zn-Zr phase diagram, the intermetallic phase Zn₂₂Zr, which corresponds to card number (03-065-6202), forms at 550°C because zirconium does not dissolve into the Zn matrix at this temperature. Because Zn has a larger concentration than Zr, the Zn phase will develop more dominantly than the Zn₂₂Zr phase, as seen by the Zn phase's higher peak height. In the highest Zn phase, the diffraction 2θ peak is 43.28°. The Zn phase also has further 2θ diffraction peaks at 36.32°, 39.04°, 43.28°, 54°, 70°, and 71° (Wątroba et al., 2018; Ghani Fahmi et al., 2020). In Fig.3d, the (Zn-0.4wt.% Zr + 0.4 wt. %Ag) alloy appears one a single phase (α - Zn) (Wa et al., 2019).



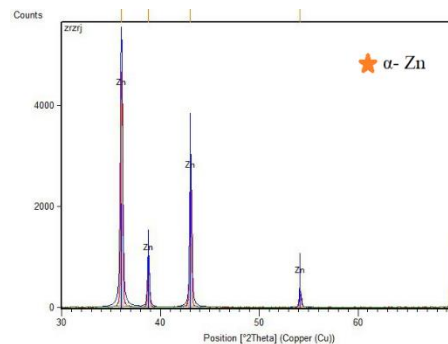
a: XRD Patterns for Zn pure alloy.



b: XRD Patterns for Zn-0.4wt% Ag.



c: XRD Patterns for Zn-0.4wt% Zr.



d: XRD Patterns for Zn-0.4wt% Ag-0.4wt% Zr

Fig.3. XRD patterns for all alloys

3.3. The micro-hardness test

Vickers hardness type (Digital Micro hardness tested HV-1000) was measured for all specimens of alloys at a load of (100g) using a fixed loading duration of (10 sec.).

Fig.4, it can be observed that the hardness value of base alloy B is less than alloys with additives where A1, A2 and A3 have higher values of hardness in comparison with it. The application of pure Zinc in biodegradable implants is largely limited by its poor mechanical qualities, such as low strength and hardness. When Ag and Zr are added, the hardness increases because of the solid solution strengthening effect that Ag dissolved in the Zn matrix causes the formation of an intermetallic phase $Zn_{22}Zr$ (Wa et al., 2019). As impurity atoms that go into solid solutions typically create lattice strains on the nearby host atoms, making the alloy stronger than the base zinc alloy. The lattice strain field interacts with these impurity atoms and dislocations, limiting the dislocations' mobility (Number & Weight, n.d.). Restricting the movement of dislocations led to an increase in hardness values. With the addition of Silver, the hardness improved, but its values are lower than alloy with the addition of Zirconium, because Zirconium is inherently hard and therefore shows more resistance than Silver in impeding the movement of dislocations. The alloy with the addition of Silver and Zirconium together, their values are the highest because a metal's strength and hardness increase as the concentration of impurity atoms that go into the solid solution increases.

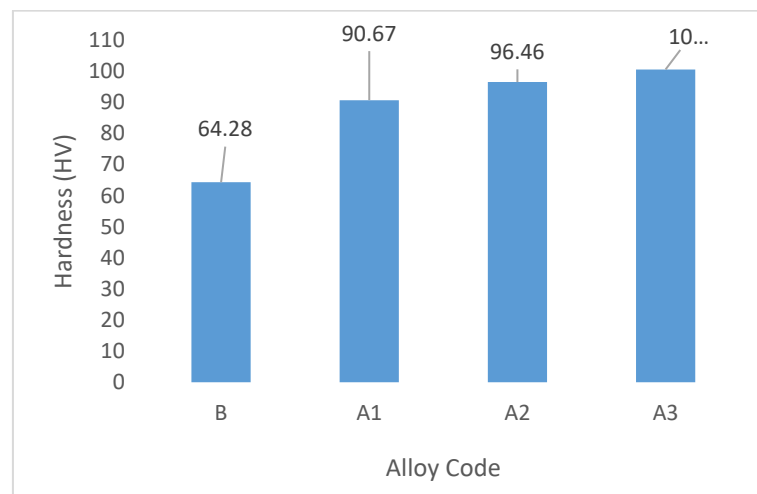


Fig. 4. effect additions of Ag and Zr on Hardness for Zn alloys

Table 2 shows the improvement percentage in the hardness values of the Zn alloys with and without additives. The improvement percentage of hardness is increased from 41% at A1 and 50% at A2 then increase to maximum (56.3%) at mixing addition of Silver and Zirconium. The highest percentage of improvement at mixing addition is because of the solid solution strengthening effect that Ag dissolved in the Zn matrix causes and the formation of an intermetallic phase $Zn_{22}Zr$ as shown in the XRD test.

Table 2 Micro-hardness and improvement percentage of all alloys

Alloy Code	Hardness (HV)	Improvement percentage%
B	64.28	-----
A1	90.67	41
A2	96.46	50
A3	100.53	56.3

3.4. Compression test

The results of the compressive strength test are illustrated in Fig.5. The strength of compressive values of the Zinc alloy with the additions Ag and Zr are higher than its value for the base alloy because of the solid solution strengthening effect that Ag dissolved in the Zn matrix causes the formation of an intermetallic phase Zn₂₂Zr. The formation of the solid solution with an intermetallic phase Zn₂₂Zr in the addition of Zirconium or Silver, or adding them to base alloy together led to difficulty in sliding of the atomic levels by impeding the movement of the dislocations, where interactions exist between impurity atoms and dislocations that are in motion during plastic deformation. Thus, greater applied stress is necessary first to initiate and then continue plastic deformation for alloy (Number & Weight, n.d.).

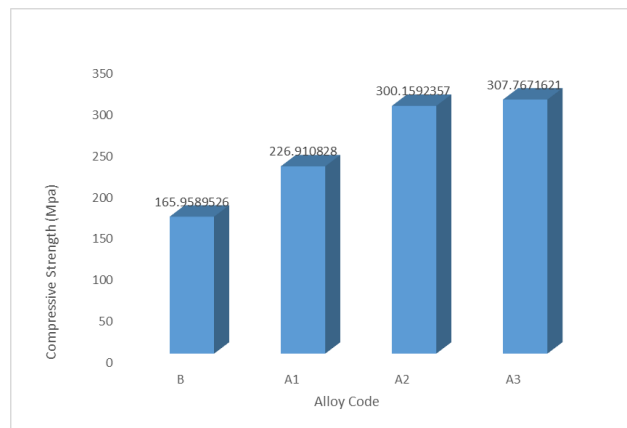


Fig.5 Compressive strength for all alloys

Table 3 demonstrates the compressive strength magnitudes and improvement percentage of alloys with and without additives. Compared with 165.95MPa for the base alloy, A1 has 226.91 MPa and 36.73% as improvement percentages while A2 and A3 alloys have 300.15 and 307.76 MPa with improvement percentages of 80.86% and 85.45% respectively. A3 alloy is considered the best addition for Zn alloy to enhance compressive strength where it achieves a higher improvement percentage.

Table 3 The compressive strength and improvement percentage of all alloys

Alloy code	Compressive strength(MPa)	Improvement percentage %
B	165.95	-----
A1	226.91	36.73
A2	300.15	80.86
A3	307.76	85.45

4. CONCLUSIONS AND RECOMMENDED

Newly created Zn-based binary and ternary alloys have been examined in this work. The objective was to assess if pure zinc's subpar mechanical qualities might be improved. These alloys' microstructure and mechanical characteristics were detailed for the first time. Given the limits of in vitro studies, the following inferences may be made from the data that have been presented: The hardness value of zinc based alloy is (64.28 kg/mm²) increased to (100.53kg/mm²) for (Zn-Ag-Zr) alloy. The highest percentage of improvement at mixing addition is because of the solid solution strengthening effect that Ag dissolved in the Zn matrix causes and the formation of an intermetallic phase Zn₂₂Zr as shown in the XRD test. In addition, the compression value of zinc based alloy is (165.95 MPa) increased to (307.76 MPa) for (Zn-Ag-Zr) alloy, and the improvement percentage of compression test to (Zn-Ag-Zr) alloy is (85.45%). So (Zn-Ag-Zr) alloy is considered the best alloy to enhance compressive strength where achieve higher improvement percentage. The findings clearly show that the materials under investigation, particularly the ternary (zinc + 0.4 silver + 0.4 zirconium) alloy, can be regarded as a potential biodegradable metallic material for fracture fixations or stents. I hope that this paper open new horizons to the fabrication of another Zinc based alloys with rare elements or another percentages to use it in the clinical applications.

5. REFERENCES

- Ag-, C., Statements, B., & Pycnometer, W. (2015). Standard Test Method for iTeh Standards iTeh Standards. i, 22–25. <https://doi.org/10.1520/F3306-19.1>
- Dargusch, M. S. (2019). Acta Biomaterialia The influence of alloying and fabrication techniques on the mechanical properties , biodegradability and biocompatibility of zinc : A comprehensive review. Acta Biomaterialia, 87, 1–40. <https://doi.org/10.1016/j.actbio.2019.01.035>
- Ghani Fahmi, M. W., Trinanda, A. F., Pratiwi, R. Y., Astutiningtyas, S., & Zakiyuddin, A. (2020). The Effect of Zr Addition on Microstructures and Hardness Properties of Zn-Zr Alloys for Biodegradable Orthopaedic Implant Applications. IOP Conference Series: Materials Science and Engineering, 833(1). <https://doi.org/10.1088/1757-899X/833/1/012065>
- Gu, X., Zheng, Y., Cheng, Y., Zhong, S., & Xi, T. (2009). Biomaterials In vitro corrosion and biocompatibility of binary magnesium alloys. Biomaterials, 30(4), 484–498. <https://doi.org/10.1016/j.biomaterials.2008.10.021>

- Guillory, R. J., Mostaed, E., Oliver, A. A., Morath, L. M., Earley, E. J., Flom, K. L., Kolesar, T. M., Mostaed, A., Summers, H. D., Kwesiga, M. P., Drelich, J. W., Carlson, K. D., Dragomir-Daescu, D., & Goldman, J. (2022). Improved biocompatibility of Zn–Ag-based stent materials by microstructure refinement. *Acta Biomaterialia*, 145, 416–426. <https://doi.org/10.1016/j.actbio.2022.03.047>
- Haleem, A. H., Radhi, N. S., Jaber, N. T., & Al-Khafaji, Z. (2024). Preparation and Exploration of Nano-Multi-Layers on 316l Stainless Steel for Surgical Tools. *Jordan Journal of Mechanical and Industrial Engineering*, 18(2), 339–350. <https://doi.org/10.59038/jjmie/180207>
- Hermawan, H. (2018). Updates on the research and development of absorbable metals for biomedical applications. *Progress in Biomaterials*, 7(2), 93–110. <https://doi.org/10.1007/s40204-018-0091-4>
- Jasim, A. H., & Radhi, N. S. (2024). Review on Improvement the Turbine Oxidation and Hot Resistant against Corrosion by Nickel – Based Superalloy. 89–104. <https://doi.org/10.52209/2706-977X>
- Kabir, H., Munir, K., Wen, C., & Li, Y. (2021). Bioactive Materials Recent research and progress of biodegradable zinc alloys and composites for biomedical applications : Biomechanical and biocorrosion perspectives. *Bioactive Materials*, 6(3), 836–879. <https://doi.org/10.1016/j.bioactmat.2020.09.013>
- Kong, L., Heydari, Z., Lami, G. H., Saberi, A., Baltatu, M. S., & Vizureanu, P. (2023). A Comprehensive Review of the Current Research Status of Biodegradable Zinc Alloys and Composites for Biomedical Applications. *Materials*, 16(13). <https://doi.org/10.3390/ma16134797>
- Levy, G. K., Goldman, J., & Aghion, E. (2017). The prospects of zinc as a structural material for biodegradable implants—a review paper. *Metals*, 7(10), 1–18. <https://doi.org/10.3390/met7100402>
- Liu, X., Sun, J., Qiu, K., Yang, Y., Pu, Z., Li, L., & Zheng, Y. (2016). Effects of alloying elements (Ca and Sr) on microstructure, mechanical property and in vitro corrosion behavior of biodegradable Zn-1.5Mg alloy. *Journal of Alloys and Compounds*, 664, 444–452. <https://doi.org/10.1016/j.jallcom.2015.10.116>

- Ma, J., Zhao, N., & Zhu, D. (2015). Endothelial Cellular Responses to Biodegradable Metal Zinc. *ACS Biomaterials Science and Engineering*, 1(11), 1174–1182. <https://doi.org/10.1021/acsbiomaterials.5b00319>
- Mostaed, E., Mostaed, A., Beanland, R., Mantovani, D., & Vedani, M. (2017). PT. *Materials Science & Engineering C*. <https://doi.org/10.1016/j.msec.2017.04.023>
- Mostaed, E., Sikora-Jasinska, M., Drelich, J. W., & Vedani, M. (2018). Zinc-based alloys for degradable vascular stent applications. *Acta Biomaterialia*, 71, 1–23. <https://doi.org/10.1016/j.actbio.2018.03.005>
- Number, A., & Weight, A. (n.d.). No Title.
- Okab, B. A., Salman, J. M., & Radhi, N. S. (n.d.). ZINC ALLOYS AS TEMPORARY BIOMEDICAL IMPLANTS : A REVIEW. 1–21.
- Okamoto, H. (2007). Zn-Zr (Zinc-Zirconium). *Journal of Phase Equilibria and Diffusion*, 28(2), 236–237. <https://doi.org/10.1007/s11669-007-9043-8>
- Pierson, D., Edick, J., Tauscher, A., Pokorney, E., Bowen, P., Gelbaugh, J., Stinson, J., Getty, H., Lee, C. H., Drelich, J., & Goldman, J. (2012). A simplified in vivo approach for evaluating the bioabsorbable behavior of candidate stent materials. *Journal of Biomedical Materials Research - Part B Applied Biomaterials*, 100 B(1), 58–67. <https://doi.org/10.1002/jbm.b.31922>
- Radhi, N. S., Kareem, N. E., Al-Khafaji, Z. S., Sahi, N. M., & Falah, M. W. (2022). Investigation Biological and Mechanical Characteristics of Hybrid PMMA Composite Materials as Prosthesis Complete Denture. *Egyptian Journal of Chemistry*, 65(10), 681–688. <https://doi.org/10.21608/EJCHEM.2022.110545.5034>
- Sabir, M. I., Xu, X., & Li, L. (2009). A review on biodegradable polymeric materials for bone tissue engineering applications. *Journal of Materials Science*, 44(21), 5713–5724. <https://doi.org/10.1007/s10853-009-3770-7>
- Wa, M., Bednarczyk, W., Kawa, J., Mech, K., Marciszko, M., Boelter, G., Banzhaf, M., & Ba, P. (2019). Design of novel Zn-Ag-Zr alloy with enhanced strength as a potential biodegradable implant material. 183. <https://doi.org/10.1016/j.matdes.2019.108154>
- Wątroba, M., Bednarczyk, W., Kawalko, J., & Bała, P. (2018). Effect of zirconium microaddition on the microstructure and mechanical properties of Zn-Zr alloys. *Materials Characterization*, 142(April), 187–194. <https://doi.org/10.1016/j.matchar.2018.05.055>

Williams, M. E., Boettinger, W. J., & Kattner, U. R. (2004). Contribution to the Zr-Rich Part of the Zn-Zr Phase Diagram. *Journal of Phase Equilibria & Diffusion*, 25(4), 355–363. <https://doi.org/10.1361/15477030420124>

Xiao, X., Liu, E., Shao, J., & Ge, S. (2021). Advances on biodegradable zinc-silver-based alloys for biomedical applications. *Journal of Applied Biomaterials and Functional Materials*, 19. <https://doi.org/10.1177/22808000211062407>

Yin, Y. X., Zhou, C., Shi, Y. P., Shi, Z. Z., Lu, T. H., Hao, Y., Liu, C. H., Wang, X., Zhang, H. J., & Wang, L. N. (2019). Hemocompatibility of biodegradable Zn-0.8 wt% (Cu, Mn, Li) alloys. *Materials Science and Engineering C*, 104(February), 109896. <https://doi.org/10.1016/j.msec.2019.109896>

Zhang, M., Wang, X., Zhang, S., Wang, T., Wang, X., Liu, S., Zhao, L., & Cui, C. (2023). Fabrication and Properties of a Biodegradable Zn-Ca Composite. *Materials*, 16(19). <https://doi.org/10.3390/ma16196432>

Zheng, Y. F., Gu, X. N., & Witte, F. (2014). Biodegradable metals. 77, 1–34. <https://doi.org/10.1016/j.mser.2014.01.001>